Am J Cancer Res 2017;7(3):448-461
www.ajcr.us /ISSN:2156-6976/ajcr0050646

Original Article

Histone demethylase PHF8 promotes progression and metastasis of gastric cancer

Shuyan Li[1], Ao Sun[1], Xiuming Liang[1], Lin Ma[1], Li Shen[1], Tongyu Li[1], Lixin Zheng[1], Wenjing Shang[1], Wei Zhao[2], Jihui Jia[1]

[1]*Department of Microbiology and Key Laboratory of Infection and Immunity of Shandong Province, School of Basic Medical Science, Shandong University, Jinan 250012, Shandong, PR China;* [2]*Department of Immunology and Key Laboratory of Infection and Immunity of Shandong Province, School of Basic Medical Science, Shandong University, Jinan 250012, Shandong, PR China*

Received February 12, 2017; Accepted February 15, 2017; Epub March 1, 2017; Published March 15, 2017

Abstract: Histone demethylase plant homeodomain (PHD) finger protein 8 (PHF8) has been implicated in tumor development and malignant progression in various types of cancers. However, its potential roles in gastric cancer (GC) have not been explored. In this report, we show that PHF8 expression is upregulated in GC tissues, and the enhanced PHF8 level indicates a poor prognosis of GC patients. PHF8 knockdown reduces proliferation and metastasis of GC cells, while PHF8 overexpression has the opposite effects. Mechanistically, PHF8 interacts with β-catenin, and binds to the promoter region of vimentin, leading to the promotion of vimentin transcription. In addition, we show that *H. pylori,* the single most important risk factor for GC, markedly induce PHF8 expression. Our results suggest that *H. pylori*-induced PHF8-β-catenin-vimentin axis activation is a novel mechanism for GC malignant progression. Thus, we identify PHF8 as an oncogenic factor of GC, and suggest PHF8 might be a potential molecular target for therapeutic approaches for GC.

Keywords: PHF8, proliferation, metastasis, β-catenin, vimentin, gastric cancer, *H. pylori*

Introduction

Gastric cancer (GC) is one of the leading causes of cancer death in less-developed countries [1]. It is difficult to detect in the early stages and GC malignant progression is the main reason responsible for its poor prognosis. Based on data from Surveillance, Epidemiology, and End Results Program (SEER) 18 2006-2012, the five-year survival rate of GC patients diagnosed with Stage I was up to 66.9%. However, more than 63% of GC patients were diagnosed with metastasis. Consequently, the five-year survival rate decreased sharply to 5% (stage IV). Therefore, it is critical to elucidate the mechanism of GC initiation and metastasis and to identify novel therapeutic approaches for GC.

It is clear that histone modification patterns alteration is involved in the development and metastasis of cancer [2]. Histone demethylases, including KDM1 (Lysine (K) Demethylase1) family and Jumonji C (JmjC) domain-containing family, have been linked to cancer [3]. For instance, LSD1 inhibits breast cancer metastasis, but promotes proliferation, migration and invasion of non-small cell lung cancer (NSCLC) [4, 5]. KDM5B promotes bladder and lung tumor progression, but serves as a tumor suppressor in melanoma [6, 7]. Histone demethylases play important roles during GC initiation and metastasis as well. Previously, our group has reported that RBP2 promote GC malignant transformation by inhibiting cyclin-dependent kinase inhibitors (CDKIs, including p21, p27 and p16) and enhancing cyclin D1 expression [8, 9]. RBP2 promotes GC malignant progression through TGF-β1-(p-Smad3)-RBP2-E-cadherin-Smad3 feedback circuit [10]. JMJD2B induces GC cell proliferation and promotes GC metastasis by enhancing epithelial-mesenchymal transition (EMT) through cooperating with β-Catenin [11, 12]. Other investigators also consider targeting histone demethylases as a new weapon in the

fight against cancer [3]. Thus, illustrating the role of histone demethylases in GC is critical for the treatment of GC.

Plant homeodomain (PHD) finger protein 8 (PHF8, also termed KDM7B), a JmjC-domain-containing protein, is a member of the histone demethylase family [13]. Serving as a transcription coactivator, PHF8 were shown to be involved in human cancer progression and metastasis. In breast cancer, ubiquitin-specific protease 7 (USP7)-mediated stabilization of PHF8 regulated cyclin A2 expression to promote carcinogenesis [14]; PHF8 upregulated SNAI1 and ZEB1 to induce an EMT-like process and contributed to MYC-induced cell proliferation [15]. In human prostate cancer, it was shown that PHF8 promoted cellular transformation and survival by regulating oncomiR miR-125b [16]; PHF8 also contributed to cancer progression through hypoxia-inducible factor (HIF)/PHF8/androgen receptor (AR) axis and induced drug resistance in castration-resistant prostate cancer (CRPC) [17]. In laryngeal and hypopharyngeal squamous cell carcinoma (LHSCC), PHF8 was upregulated and associated with adverse prognosis [18]. However, the mechanistic insights into the role of PHF8 in GC progression and matastasis remain to be investigated.

In the present study, we show that the histone demethylase PHF8 is upregulated in GC and correlates with poor prognosis of GC. PHF8 enhances metastasis and progression of GC in vitro and in vivo. Mechanistically, PHF8 regulates the expression of EMT related genes, such as vimentin. PHF8 interacts with β-catenin and bind to the promoter region of vimentin, leading to the enhancement of vimentin transcription. Thus, we identify PHF8 as an oncogenic protein in GC, and suggest that PHF8 might be a potential therapeutic target for preventing GC progression.

Methods and materials

Cell cultures

GES-1, BGC-823, HGC-27, MGC-803 and SGC-7901 cells were cultured in RPMI-1640 (Gibco, Carlsbad, CA, USA) supplemented with 10% fetal bovine serum (FBS, Gibco, Carlsbad, CA, USA). AGS cells were cultured in F12 (HyClone, USA) supplemented with 10% FBS. BGC-823 cells stably knocking down PHF8 were selected using 2 μg/ml puromycin (Gibco, Carlsbad, CA, USA).

Reagents, siRNA and plasmids transfection

Lipofectamine 2000 (Invitrogen, Carlsbad, CA, USA) was used for stable transfection of PHF8 shRNA (GenePharma, Shanghai, China) and transient silencing of PHF8 siRNA (Sigma-Aldrich, St Louis, MO, USA) according to the manufacturer's protocol. Target sequence of PHF8 for transient silencing was 5'-CCAATC-TGACTCTCTTTGA-3'. Roche Transfection Reagent (Roche, Basel, Switzerland) was used for transient transfction of PHF8 plasmid and catalytically inactive H247A mutant plasmid according to the manufacturer's protocol. PHF8 plasmid and catalytically inactive H247A mutant plasmid were kindly donated by Prof. Liu Wen (University of Xiamen, Xiamen, China).

H. pylori cultures and a mouse model of H. pylori infection

The *H. pylori* strains *26695* and *SSI* were grown in Brucella broth supplemented with 5% FBS under microaerophilic conditions (5% O_2, 10% CO_2, and 85% N_2) at 37°C. The bacteria were collected through centrifugation, quantified according to OD600 and added to cell cultures with multiplicity of infection (MOI) at 100 immediately. The mouse model of *H. pylori* infection was performed as described preciously [19]. All animal experiments were approved by Shandong University Research Ethics Committee.

Clinical samples

For IHC, 77 cases of GC and 46 cases of adjacent non-cancer tissues were acquired from Shanghai Outdo Biotech Co., Ltd. (Shanghai, China). 37 samples of atrophic gastritis (AG) with *H. pylori* positive or negative were obtained from Jinan Central Hospital, Shandong, P. R. China. *H. pylori* infection in patients with AG was detected by a 13C urea breath test. For western blot analysis, eight pairs of GC and matched adjacent non-tumor gastric tissues were frozen and stored in liquid nitrogen until use. For qRT-PCR, 40 cases of AG samples were obtained from Jinan Central Hospital, Shandong, PR China. The samples were stored in RNAlater (QIAGEN, Germany) at -80°C until use for RNA extraction. The clinical stages and

histological types of the tumors were defined according to WHO classification criteria. All clinical samples were approved for analysis by Shandong University Research Ethics Committee.

Proliferation and metastasis assays in vivo

Female thymus-null BALB/c nude mice were obtained from the Mu Tu Biological Technology Co., Ltd. (Nanjing, China). For proliferation assay, BGC-823 cells (3×10^5) that stably transfected with PHF8 shRNA or negative control were subcutaneously injected into the right and left flank of 5 nude mice, respectively. Tumor growth was measured every four days. The mice were sacrificed after 20 days later. For metastasis assay, BGC-823 cells (4×10^5) that stably transfected with PHF8 shRNA or negative control were intravenously injected via tail vein of nude mice. The lungs were harvested after one month and stored at formalin for further HE staining.

IHC

IHC was performed according to a standard procedure. Briefly, formalin-fixed, paraffin-embedded (FFPE) sections obtained from mouse or patient samples were subjected to deparaffination and dehydration. After antigen retrieval with 15 minutes heat treatment in 10 mM sodium citrate and 30% H_2O_2 treatment, the sections were blocked in goat serum for 30 min. Then the sections were incubated with specific primary antibodies against PHF8 (1:200, Abcam, Cambridge, MA, USA), and vimentin (1:200, Cell Signaling Technology, Danvers, MA, USA) overnight at 4°C. Finally, we incubated the sections with corresponding secondary antibodies and detected the staining using a DAB staining kit (Vector Laboratories, Burlingame, CA, USA). The intensity of positive staining was scored as follows: 0, no immunostaining; 1, light brown color; 2, medium brown color; and 3, dark brown color. The percentage of positively stained cells was scored as follows: 0, 0%; 1, < 25%; 2, 25-75%; 3, > 75%. We got the IHC score by multiplying these two scores. High expression: IHC score ≥ 5; low expression: IHC score < 5.

Colony formation assay

Cells (500 cells/well) were seeded in 6-well plates and incubating for 7-12 days. The cells were fixed using methanol and stained with Giemsa. The number of colonies containing more than 100 cells was counted for the subsequent analysis.

Wound healing and migration assays

For wound healing assay, 6-well plate were seeded with cells and cell surface was scratched using a pipette tip. At 0, 24, 48 and 72 hours, accurate wounds measurement were performed to calculate the healing area. The wound closure area = [(wound length at 0 hour)-(wound length at 24, 48 and 72 hours)] × (wound width). For migration assay, 50000 GC cells were loaded into upper chamber of collagen-coated Transwells for 24 or 48 hours. Lower chamber was loaded with medium containing 20% FBS. The cells migrated to the lower well were fixed using methanol and stained with Giemsa. Cells were calculated with an inverted microscope. All experiment were performed with 3 replicates.

qRT-PCR

TRIzol reagent (Invitrogen, Carlsbad, CA, USA) was used to extract total RNA according to the manufacturer's protocol. Random primers and MMLV reverse transcriptase (Fermentas, Canada) were used to synthesize cDNA. qRT-PCR analysis performed with SYBR-Green qRT-PCR assays (TaKaRa, Japan). β-actin expression was used to normalize data. Primers used for qRT-PCR assays were shown as below: 5'-AGTTGCGTTACACCCTTTCTTG-3' and 5'-CACCTTCACCGTTCCAGTTTT-3' for β-actin; 5'-AGTCACCGCATAGTCAGGCA-3' and 5'-CCTCTGTTTCTGCCCAGCTT-3' for PHF8; 5'-GGACCAGCTAACCAACGACA-3' and 5'-AAGGTCAAGACGTGCCAGAG-3' for vimentin.

Western blot

Protein lysis buffer containing phosphatase and protease inhibitors were used to lyse cells. Equal amounts of extracts were resolved on SDS-PAGE and transferred to PVDF membranes, blocking with 5% nonfat dry milk and subsequently incubated with primary antibodies and then with the corresponding secondary antibodies. Millipore ECL regents were used to detect immunoblot signals. Anti-PHF8 was from Abcam (Cambridge, MA, USA). Anti-β-actin was from Sigma-Aldrich (St Louis, MO, USA).

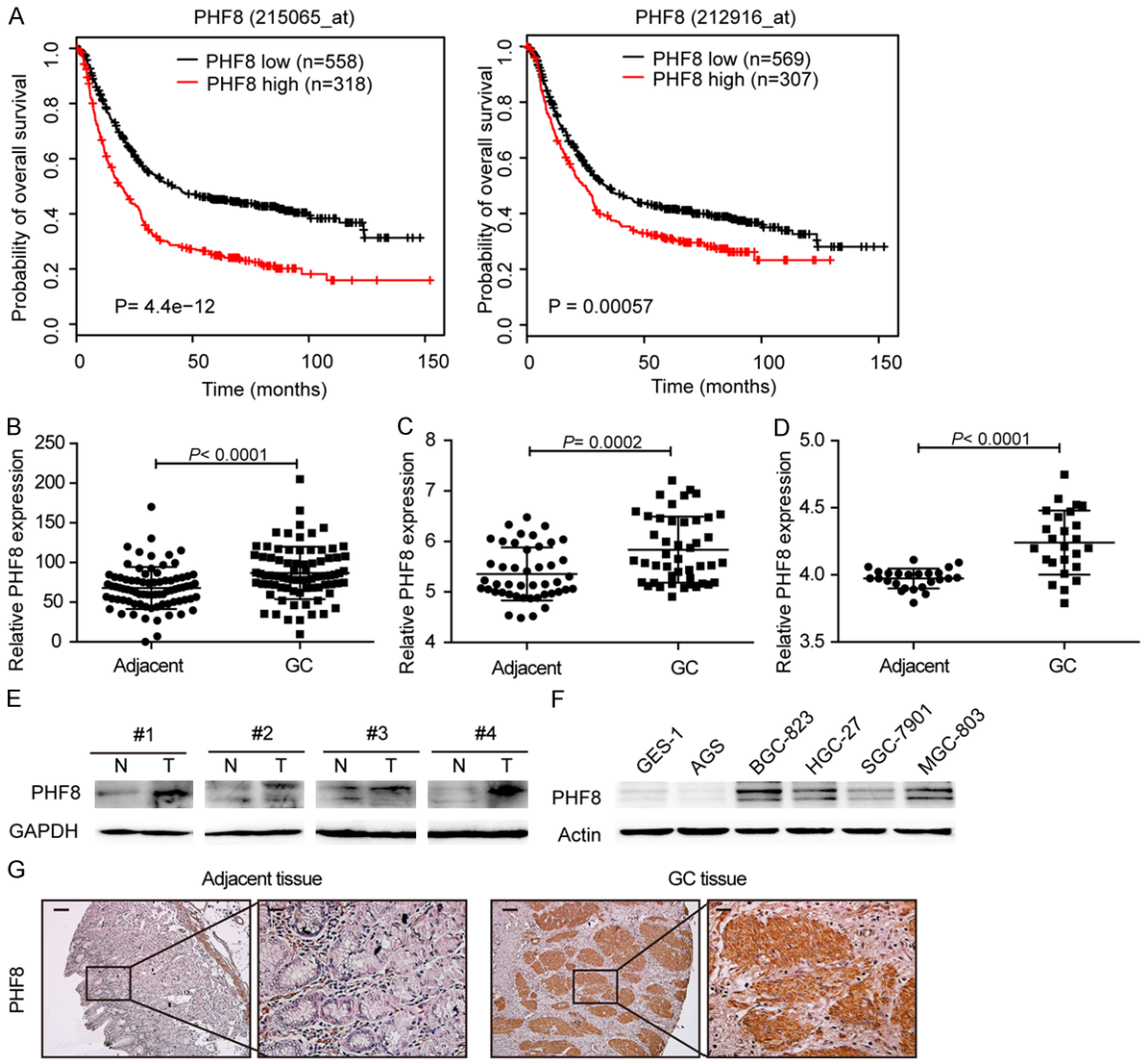

Figure 1. Enhanced PHF8 level correlates with poor GC prognosis. A. Kaplan-Meier analysis of two probes of PHF8 (left: 215065_at; right: 212916_at) in survival of GC patients (log-rank test; n = 876). The data and P-values were obtained from the Kaplan-Meier Plotter database. B. PHF8 mRNA expression in 80 pairs of GC and adjacent normal tissues. The data were obtained from the GEO database (GSE27342). C. PHF8 mRNA expression in 45 pairs of GC and adjacent normal tissues. The data were obtained from the GEO database (GSE63089). D. PHF8 mRNA expression in 25 pairs of GC and adjacent normal tissues. The data were obtained from the GEO database (GSE13195). E. Western blot analysis of PHF8 in four pairs of GC tissues (T) and corresponding normal tissues (N). F. Western blot analysis of PHF8 in four poor differentiated or undifferentiated GC cell lines (BGC-823, HGC-27, SGC-7901 and MGC-803) and normal gastric mucous membrane epithelial cell line (GES-1) and a moderately differentiated GC cell line (AGS). G. IHC staining for PHF8 in GC and adjacent normal tissues. Scale bars, 200 μm (insets 25 μm).

Anti-vimentin, anti-ZEB-1, anti-Slug, anti-ZO-1 and anti-E-cadherin were from Cell Signaling Technology (Danvers, MA, USA). Anti-Flag and Anti-HA were from Proteintech (Rosemont, IL, USA).

ChIP

The SimpleChIP® Enzymatic Chromatin IP Kit (Cell Signaling, Danvers, MA, USA) was used to perform Chromatin immunoprecipitation (ChIP) assays according to the manufacturer's standard protocol. Chromatin fragments derived from BGC-823 cells were immunoprecipitated with 5 μg PHF8 antibody.

Immunoprecipitation (IP) assay

Pierce™ Co-Immunoprecipitation Kit (Thermo-Fisher, Waltham, MA, USA) was used to perform

Ip/Co-IP assays according to the manufacturer's standard protocol. BGC-823 cells lysates were incubated with 5 μg PHF8 antibody or HA antibody.

Luciferase reporter assay

Vimentin promoter wild and mutant plasmids were kindly provided by Dr. Christine Gilles (University of Liege, Liege, Belgium). Vimentin promoter wild or mutant plasmids and the internal control vector pRL-TK, which expresses renilla luciferase, were co-transfected into BGC-823 cells using Roche Transfection Reagent (Roche, Basel, Switzerland) according to the manufacturer's protocol. 48 hours later, luciferase assays were performed using a Luciferase Assay System (Promega, Madison, WI, USA) according to the manufacturer's instructions.

Statistical analysis

Data of experiment groups are represented as the mean ± SD and significant differences were analyzed using two-tailed Student's *t* tests or Mann-Whitney U-test. Statistical analyses were performed using GraphPad PRISM version 6.01. The relationships of PHF8 expression and clinicopathologic features of GC patients were analyzed by the χ^2 test using the SPSS version 23.0. Values of *P* less than 0.05 were considered as statistically significant.

Results

Enhanced PHF8 level correlates with poor GC prognosis

To identify novel histone demethylase, which correlates with the prognosis of GC, we performed a bioinformatics analysis of histone demethylase expression profiles from 876 GC patients using Kaplan-Meier Plotter, a meta-analysis based biomarker assessment tool [20]. The correlation between overall survivals with the gene expression levels of comprehensive list of histone demethylases was examined. We found that high expression of two enzymes, KDM5C and PHF8, correlated with significant poor overall survival in GC (**Figure 1A** and Table S1). It has been reported that KDM5C promotes GC cells proliferation and invasion [21]. Therefore, we focused on PHF8 and investigated possible link between enhanced PHF8 expression and GC progression.

To investigate the potential roles of PHF8 in progression of GC, we analyzed public microarray data from GEO repository (GSE27342, GSE63089 and GSE13195) and found that PHF8 expression was significantly increased in GC compared with adjacent normal tissues (**Figure 1B-D**). Western blot analysis confirmed that PHF8 protein expression was significantly enhanced in four GC samples paired with adjacent non-tumor tissues (**Figure 1E**). PHF8 protein expression level was markedly increased in four poor differentiated or undifferentiated GC cell lines (BGC-823, HGC-27, SGC-7901 and MGC-803), compared with that in GES-1 (a normal gastric mucous membrane epithelial cell line) and AGS (a moderately differentiated GC cell line) (**Figure 1F**). Consistently, immunohistochemistry (IHC) staining also showed PHF8 overexpression in GC samples compared with adjacent non-tumor tissues (**Figure 1G**). Collectively, theses results provide strong evidence that PHF8 expression is markedly upregulated in GC and correlates with GC prognosis.

PHF8 promotes cell growth and metastasis of GC in vivo

To investigate the biological role of PHF8 in GC progression, BGC-823 cells were stably transfected with PHF8 shRNA and the endogenous PHF8 expression was greatly suppressed (**Figure 2A**). First, to evaluate the role of PHF8 in cell growth, BGC-823 cells with PHF8 knockdown were subcutaneously injected into nude mice. The tumors formed by PHF8-konckdown BGC-823 cells were smaller, in both size and weight, than the negative control tumors (**Figure 2B-D**). These data showed that PHF8 promoted tumor growth *in vivo*, indicating that PHF8 could promote GC tumorigenesis *in vivo*.

Next, to evaluate the role of PHF8 in tumor metastasis, PHF8 stably knockdown cells were injected into tail vein of nude mice. One month later, the ratio of tumor metastasis in lungs from mice injected with PHF8-konckdown BGC-823 cells was 56% (5/9), while that from mice injected with negative control BGC-823 cells was 86% (6/7). Furthermore, the number of metastasis in PHF8-konckdown group was also markedly decreased (**Figure 2E** and **2F**). HE staining showed that the number of metastatic nodules in lungs from PHF8-konckdown group was significantly reduced, compared with that from negative control group (**Figure 2E**, lower lanel). Taken together, these data showed that PHF8 promoted metastasis of GC *in vivo*.

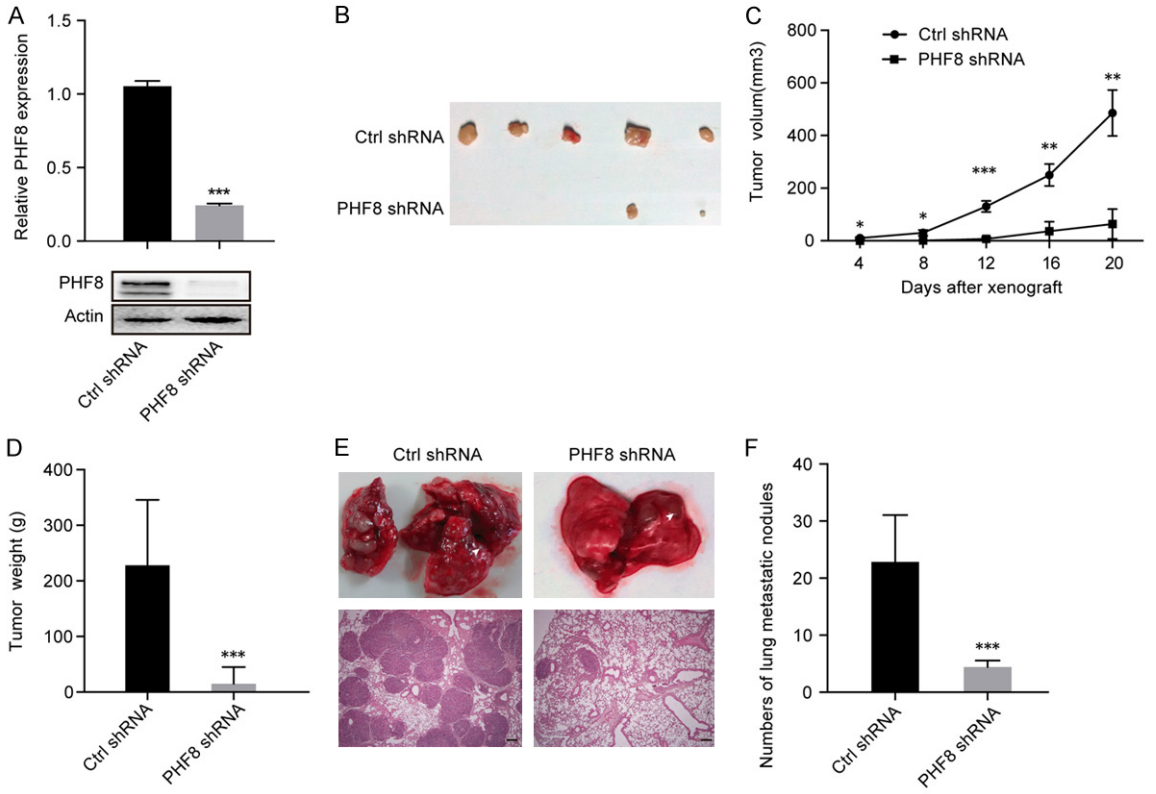

Figure 2. PHF8 promotes GC cells growth and metastasis *in vivo.* (A) qRT-PCR and Western blot analysis of PHF8 in BGC-823 cells transfected with PHF8 shRNA. (B-D) Xenograft model in nude mice. Primary tumor appearance (B), tumor growth curves (C) and the average tumor weight (D) in each group. (E) Lung metastasis in nude mice. Arrows indicate the metastatic colonization of GC cells in the lung tissues (upper panel). HE staining of lung tissues. Scale bars, 200 μm. (F) The number of lung metastatic nests in each group was counted under a low power field and is presented as the mean ± SD.

PHF8 promotes cell proliferation and migration of GC in vitro

To further examine the biological roles of PHF8 in cells proliferation and migration of GC in vitro, we performed clone formation, wound healing and transwell assays. In consistence with *in vivo* results, PHF8 knockdown decreased colony formation of GC cells, while PHF8 overexpression had the opposite effects (**Figure 3A** and **3B**). The wound healing assay demonstrated that decreased PHF8 expression in BGC-823 cells was associated with slower would closure (**Figure 3C** and **3D**). Transwell assays showed that PHF8 knockdown decreased cells invasive activity, while PHF8 overexpression increased cell migration (**Figure 3E** and **3F**). Thus, PHF8 can promote cell proliferation and migration of GC.

PHF8, as a histone demethylase, could remove methylation from H3K9me2. However, PHF8 H247A mutant, in which a histidine (H) to alanine (A) point mutation was introduced, lost the demethylase activity [22]. In order to determine whether PHF8 promotes proliferation and migration via its demethylase activity, the catalytically inactive mutant PHF8 H247A was transfected into GC cells. Colony formation and transwell assay showed that increased colony number and migrated cells after PHF8 expression were reduced in GC cells with PHF8 H247A overexpression (**Figure 3B** and **3F**). Taken together, these data indicate that PHF8 promotes cell proliferation and migration, at least partially, via its demethylase activity.

PHF8 is recruited to the vimentin promoter through physically associated with β-catenin

Next, we investigated the effects of PHF8 on the expression of several molecular markers. E-cadherin and ZO-1 (epithelial markers) dramatically increased while Slug, ZEB-1 and

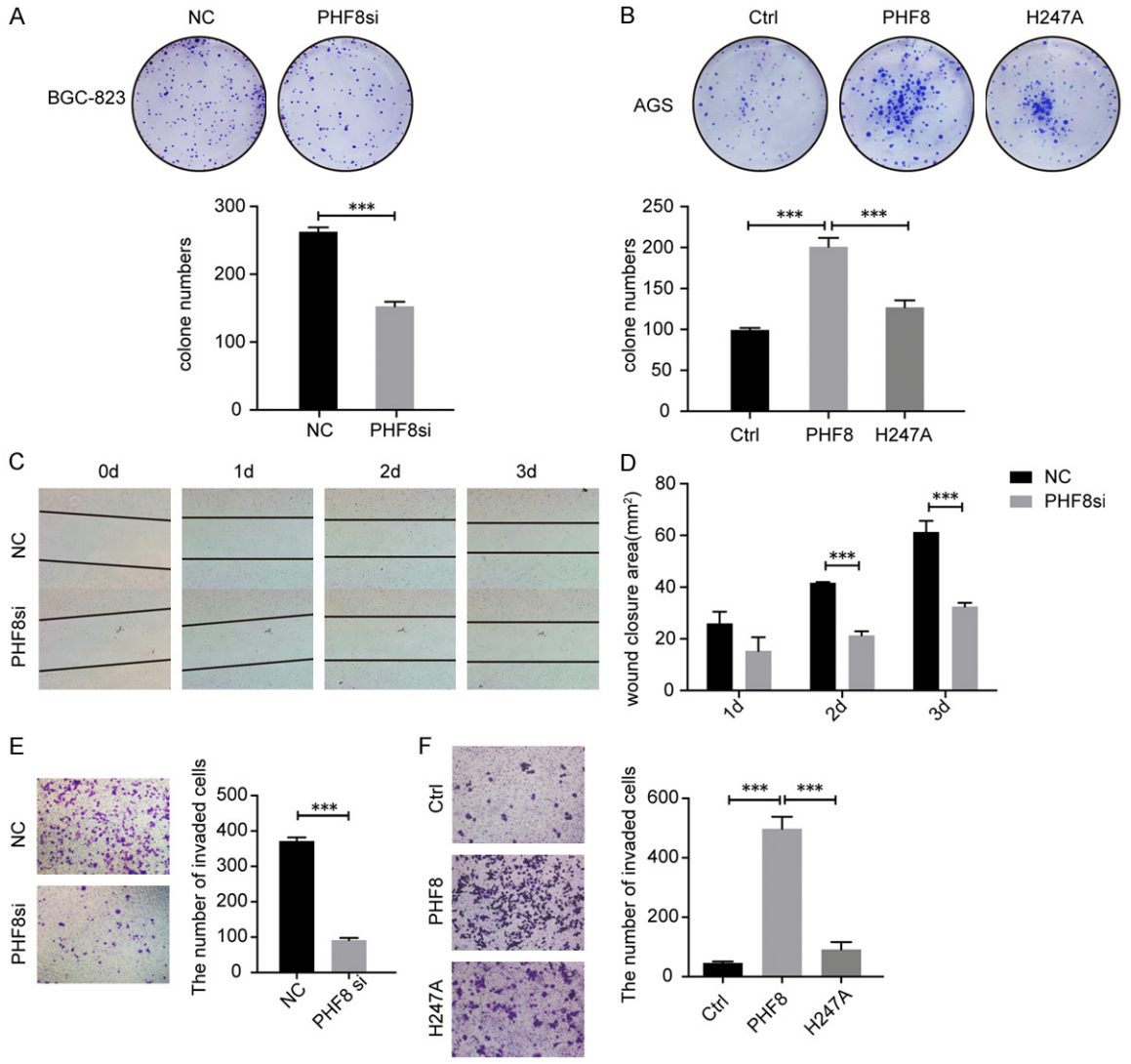

Figure 3. PHF8 promote GC cells proliferation and invasion *in vitro.* (A) Representative images (upper panel) and quantification (lower panel) of negative control (NC)- or PHF8 siRNA-transfected BGC-823 cells analyzed in a colony formation assay. (B) Representative images (upper panel) and quantification (lower panel) of control (Ctrl)- or PHF8 expression plasmid- or H247A mutant plasmid-transfected AGS cells analyzed in a colony formation assay. (C, D) Representative images (C) and quantification (D) of negative control (NC)- or PHF8 siRNA-transfected BGC-823 cells analyzed in a wound healing assay. (E) Representative images (left panel) and quantification (right panel) of negative control (NC)- or PHF8 siRNA-transfected BGC-823 cells analyzed in a transwell assay. (F) Representative images (left panel) and quantification (right panel) of control (Ctrl)- or PHF8 expression plasmid- or H247A mutant plasmid-transfected AGS cells analyzed in a transwell assay.

vimentin (mesenchymal markers) markedly decreased in PHF8 siRNA-transfected BGC-823 cells (**Figure 4A**). Consistently, PHF8 overexpression had the opposite effects (**Figure 4B**). In addition, PHF8 H247A mutant overexpression lost the regulatory effects on the expression of epithelial markers and mesenchymal markers in GC cells (**Figure 4B**). Thus, PHF8 has important roles in regulating the expression of epithelial and mesenchymal markers in GC cells.

Analysis of public microarray data from GEO repository (GE063089) showed that PHF8 expression was positively correlated with vimentin, ZEB-1 and Slug in 45 pairs of GC and corresponding normal tissues. The R (coefficient of correlation) value of viemrntin, ZEB-1, Slug with PHF8 respectively was 0.5501, 0.5117, 0.4690, indicating vimentin was the most probable target gene of PHF8 (**Figure 4C-E**). Thus, we next investigated the mechanism by which PHF8 enhanced vimentin expression. As shown

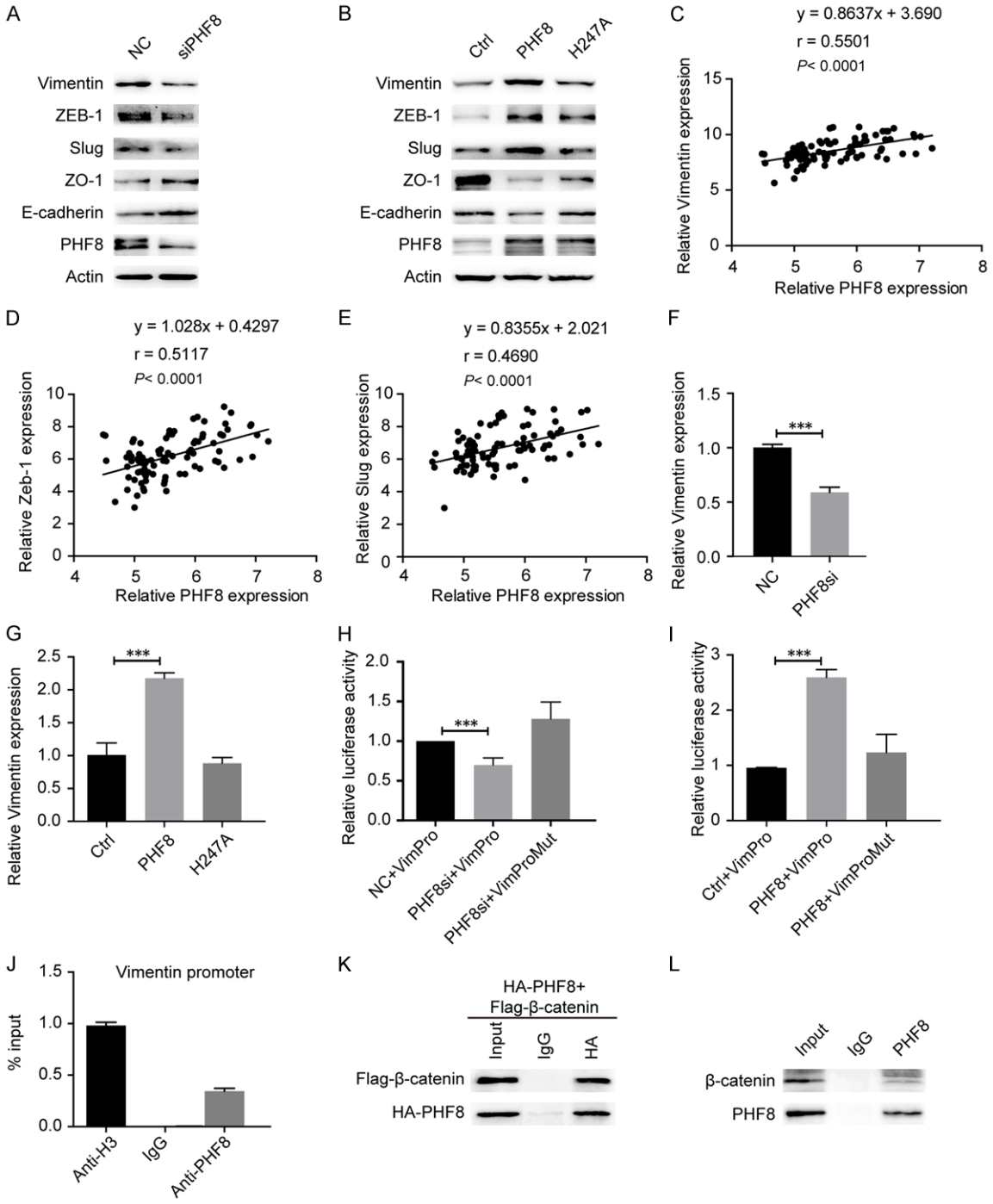

Figure 4. PHF8 is recruited to the vimentin promoter through physically associated with β-catenin. (A, B) Western blot analysis of epithelial markers (E-cadherin, ZO-1) and mesenchymal markers (Slug, ZEB-1, vimentin) in negative control (NC)- or PHF8 siRNA-transfected (I) and control (Ctrl)- or PHF8 expression plasmid- or H247A mutant plasmid-transfected (J) BGC-823 cells. (C-E) Correlation of vimentin, ZEB-1 and Slug with PHF8 mRNA expression in 45 pairs of GC and adjacent normal tissues. The data were obtained from the GEO database (GSE63089). (F, G) qRT-PCR analysis of PHF8 mRNA expression in negative control (NC)- or PHF8 siRNA-transfected (F) and control (Ctrl)- or PHF8 expression plasmid- or H247A mutant plasmid-transfected (G) BGC-823 cells. (H, I) BGC-823 cells were transfected with vimentin wild or β-catenin binding site mutant promoter, along with negative control (NC) or PHF8 siRNA (H) and control (Ctrl) or PHF8 expression plasmid (I), and then luciferase assay was performed. (J) ChIP analysis of PHF8 binds to vimentin promoter region. (K) BGC-823 cells transfected with Flag-β-catenin and HA-PHF8 were coimmunoprecipitated with anti-HA antibody. (L) BGC-823 cell lysates were immunoprecipitated with anti-PHF8 antibody.

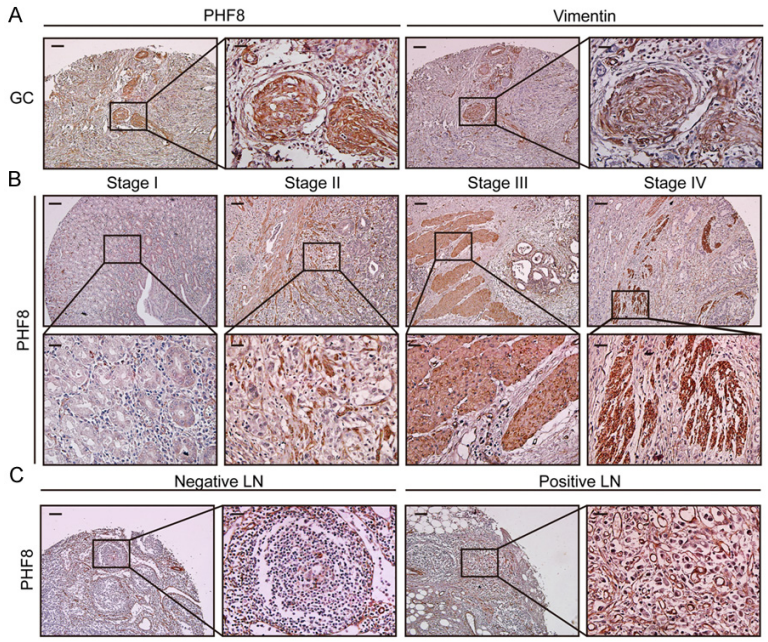

Figure 5. PHF8 expression positively correlates with metastasis in human GC. A. IHC staining for PHF8 and vimentin in GC tissues. Scale bars, 200 μm (insets 25 μm). B. IHC staining for PHF8 in GC tissues from stage I to stage IV. Scale bars, 200 μm (insets 25 μm). C. IHC staining for PHF8 in metastasis positive and negative lymph nodes. Scale bars, 200 μm (insets 25 μm).

Table 1. Association between expression of PHF8 and vimentin in GC

Variable	Total	PHF8 expression		
		Negative	Positive	*P* value[a]
Vimentin expression	77			
Negative	18	12	6	0.001
Positive	59	14	45	

Note: [a]χ^2 test.

in **Figure 4F** and **4G**, PHF8 knockdown inhibited vimentin mRNA expression, while PHF8 overexpression enhanced vimentin mRNA expression. However, PHF8 H247A mutant overexpression abolished the enhancement of vimentin expression (**Figure 4G**). PHF8 knockdown inhibited vimentin promoter luciferase activity in BGC-823 cells, while PHF8 overexpression had the opposite effects (**Figure 4H** and **4I**). Taken together, these data indicate that PHF8 promotes vimentin expression via enhancing vimentin transcription.

It has been shown that β-catenin is crucial for vimentin transcriptionally active [23]. We hypothesized a possible involvement of PHF8 and β-catenin in the transcription of vimentin. We performed a dual-luciferase assay using vimentin promoter mutant vector in which β-catenin/TCF putative binding site on the vimentin promoter were inactivated by site mutant. As a result, the mutant vector failed to be repressed or enhanced in PHF8 knockdown or overexpressed BGC-823 cells (**Figure 4H** and **4I**), indicating transcriptional regulation of vimentin by PHF8 was dependent on β-catenin. To explore whether PHF8 can interact with β-catenin physically, coimmunoprecipitation (CoIP) experiment was performed. HA-PHF8 and Flag-β-catenin plasmids were cotransfected into BGC-823 cells. The interaction between PHF8 and β-catenin was observed (**Figure 4K**). In consistent, endogenous interaction of PHF8 and β-catenin was confirmed in BGC-823 cells (**Figure 4L**). Furthermore, chromatin immunoprecipitation (ChIP) assays showed that PHF8 occupied the vimentin promoter region in BGC-823 cells (**Figure 4J**). Collectively, these results indicate that PHF8 is physically interacted with β-catenin and is recruited to the vimentin promoter, thereby facilitating the transcription of vimentin.

PHF8 expression positively correlates GC malignant progression

To unveil clinical characteristics of PHF8 expression, we collected 109 cases of tissues from GC patients. Immunohistochemical (IHC) staining showed that co-expression of vimentin and PHF8 existed in some GC samples (**Figure 5A**) and there was a significant positive correlation between expression of vimentin and PHF8 in 77 cases of gastric cancer ($P = 0.001$, **Table 1**). As expected, PHF8 expression in stage I GC was relatively low, and its expression was slightly upregulated in Stage II and III (**Figure 5B**). However, PHF8 was significantly enhanced in Stage IV (metastatic GC) (**Figure 5B**). Furthermore, PHF8 expression in metastatic lymph nodes was markedly increased com-

Table 2. Correlation between PHF8 expression and clinicopathologic features in GC patients

Characteristic	Total	PHF8 expression		
		Negative	Positive	*P* value[a]
Gender	77			
Men	54	19	35	0.687
Women	23	7	16	
Age (years)	77			
≤ 60	36	12	24	0.94
> 60	41	14	27	
Tumor size	74[b]			0.003
≤ 4	30	16	14	
> 4	44	9	35	
Differentiation	77			
Well	20	9	11	0.254
Poor	57	16	41	
pT status	72[b]			
Tis+1	9	7	2	0.002
2	9	4	5	
3	42	11	31	
4	12	3	9	
pN status	75[b]			0.002
0	24	14	10	
1	16	7	9	
2	16	4	12	
3	19	1	18	
pM status	77			0.044
pM0	63	25	38	
pM1	14	1	13	
pTNM status	77			0.002
I	15	9	6	
II	21	11	10	
III	27	5	22	
IV	14	1	13	

NOTE: [a]χ^2 test. [b]Corresponding clinical parameters in several patients are not available.

pared with non-metastatic lymph nodes (**Figure 5C**). Correlation analysis showed that PHF8 expression was positively correlated with tumor size (P = 0.003), invasion (P = 0.002), lymph node metastasis (P = 0.002), distant metastasis (P = 0.044) and TNM stage (P = 0.002, **Table 2**). Collectively, these results confirmed the role of PHF8 in GC malignant progression.

PHF8 expression is induced by H. pylori both in vitro and in vivo

Since *H. pylori* infection is the single most important risk factor for GC [24], we investigated effect of *H. pylori* infection on PHF8 expression. Higher expression level of PHF8 expression was observed in the *H. pylori*-positive gastric mucosa (**Figure 6A**, **6B**). In addition, we explored the relation between *H. pylori* infection and enhanced PHF8 expression in gastric mucosa. *H. pylori* infection induced PHF8 mRNA expression in BGC-823 and AGS cells (**Figure 6C** and **6D**). To investigate the effect of *H. pylori* on PHF8 expression in vivo, we constructed a *H. pylori* infection mouse model in N-methyl-N-nitrosourea (MNU) treated mice [25]. MNU was used to better stimulate the chronic damage under natural conditions. Gastric mucosa was normal in the control group while MNU induced chronic inflammation. Severe atrophic mucosa was observed in mice following MNU treatment combined *H. pylori* infection. PHF8 was slightly increased in MNU group; however, its expression was markedly upregulated in the group that combined MNU treatment and *H. pylori* infection (**Figure 6E**). These results showed that *H. pylori* could induce PHF8 expression both *in vitro* and *in vivo*.

Discussion

Recently, more and more evidences have shown critical roles of histone modification in development and progression of cancer [26]. Histone lysine methyltransferase SMYD3 plays a pivotal role in the formation of Ras-driven carcinomas [27]. In addition, Histone deacetylases (HDACs) are often found deregulated in many cancers, and thus they are potential effective targets for anti-tumor therapy. For example, histone deacetylase inhibitors (HDACIs) combined with phosphatidylinositol 3-kinase inhibitors (PI3KIs) could inhibit the growth of MYC-driven tumors in vivo [28]. Histone demethylase JMJD3 is unregulated in prostate cancer and is essential for the initiation and maintenance of T-cell acute lymphoblastic leukaemia (T-ALL), Hodgkin's lymphoma [29, 30]. Here we focus on PHF8, also a member of histone demethylases, and reveal its vital roles in GC development and progression.

Activating invasion and metastasis is a hallmark of cancer [31]. Epithelial-mesenchymal transition (EMT) is a process from epithelial state toward the mesenchymal state, during which, gene expression is modified, allowing cell to adopt a migratory and invasive behavior [32]. The mesenchymal marker vimentin upreg-

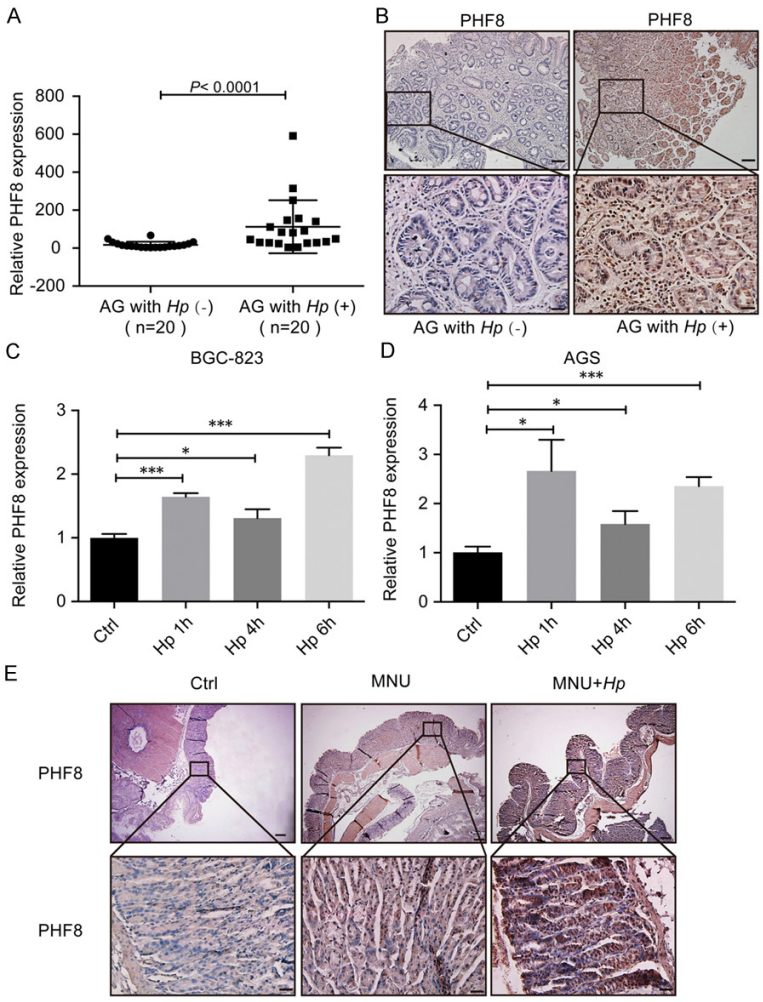

Figure 6. *H. pylori* induce PHF8 expression in vitro and in vivo. (A, B) qRT-PCR analysis (A) and IHC staining (B) of PHF8 in *H. pylori*-negative or positive AG samples. $P < 0.0001$ (Mann-Whitney U-test). Scale bars, 100 μm (insets 25 μm). (C, D) qRT-PCR analysis of PHF8 mRNA expression in *H. pylori* infected BGC-823 (C) and AGS (D) for different periods. (E) IHC staining for PHF8 in control, MNU and MNU-Hp(SSI)-infected mice. Scale bars, 200 μm (insets 25 μm).

ulation is apparently associated with the aggressive phenotype of GC [23, 33]. Our study showed that PHF8 regulated vimentin expression at the transcriptional level. Histone demethylases often regulate gene transcription by interacting with corresponding transcription factors [34-36]. IP/Co-IP verified the physical interaction of histone demethylase PHF8 and transcription factor β-catenin in GC cells. Collectively, our results reveal a novel mechanism that PHF8 promotes EMT program by promoting vimentin expression through binding to β-catenin.

β-catenin is an important transcription factor in the process of tumor invasion and progression [37]. β-Catenin/TCF4 binds directly to the promoter of ZEB1 and Slug, activates their transcription to regulate tumor invasiveness [38, 39]. Our study showed that PHF8 expression was positively correlated with the expression level of mesenchymal markers (such as Slug, ZEB-1, vimentin) in GC tissues. As we have shown, PHF8 regulates vimentin expression by interacting with β-Catenin. Thus, the PHF8/β-Catenin complex plays vital roles in the regulation of EMT-associated genes.

Sustaining proliferation signaling is one of the hallmarks of cancer as well [31]. A variety of proteins induce carcinogenesis through promoting cell proliferation. For example, RBP2 promotes GC development by inhibiting CDKIs (p21, p27 and p16) and enhancing Cyclin D1 expression [8, 9]. In our study, both in vivo and in vitro experiments showed that knocking down PHF8 expression significantly inhibited GC cell growth. And further research demonstrated that human telomerase reverse transcriptase (hTERT) expression level was markedly reduced after PHF8 downregulation (data not shown). hTERT is a major subunit of the telomerase enzyme complex which plays a critical role in regulating telomerase activity [40]. Therefore, PHF8 may promote cell proliferation through regulating telomere length by hTERT. However, the detailed mechanism needs to be further explored, which is our currently study focus.

H. pylori infection is the single most important risk factor for GC as *H. pylori*-positive individuals have at least a six-fold greater risk of devel-

oping gastric adenocarcinoma than uninfected individuals [41]. We have demonstrated *H. pylori* induced RBP2 through virulence factor CagA-PI3K/AKT-Sp1 axis contributed to GC malignant transformation [9]. *H. pylori* induced JMJD2B though β-catenin is critical for *H. pylori* induced chronic inflammation [42]. qRT-PCR and IHC analysis of *H. pylori*-positive and negative AG tissues showed that PHF8 expression was correlated with *H. pylori* infection status. Both in vitro and in vivo experiments showed that PHF8 expression could be induced by *H. pylori.*

Conclusions

In summary, our study proves that PHF8 acts as an oncogenic regulator, at least partially dependent on its histone demethylase activity. PHF8 is upregulated in GC and its overexpression is associated with proliferation and metastatic phenotype, predicting poor prognosis in GC patients. *H. pylori*-induced PHF8 binds to promoters of EMT related genes, such as vimentin, through interacting with β-catenin Thus, we identify a novel mechanism for GC malignant preogression and suggest PHF8 as an attractive target for prevention and treatment of GC.

Acknowledgements

This work was supported by the National Natural Science Foundation of China (Nos. 8157-1960, 81371781, 81372680, 81471991 and 81501720).

Disclosure of conflict of interest

None.

Address correspondence to: Dr. Jihui Jia, Department of Microbiology and Key Laboratory of Infection and Immunity of Shandong Province, School of Basic Medical Science, Shandong University, Jinan 250012, Shandong, PR China. Tel: 086-531-88382672; Fax: 086-531-88382502; E-mail: jiajihui@sdu.edu.cn

References

[1] Torre LA, Bray F, Siegel RL, Ferlay J, Lortet-Tieulent J and Jemal A. Global cancer statistics, 2012. CA Cancer J Clin 2015; 65: 87-108.

[2] Seligson DB, Horvath S, McBrian MA, Mah V, Yu H, Tze S, Wang Q, Chia D, Goodglick L and Kurdistani SK. Global levels of histone modifications predict prognosis in different cancers. Am J Pathol 2009; 174: 1619-1628.

[3] Hojfeldt JW, Agger K and Helin K. Histone lysine demethylases as targets for anticancer therapy. Nat Rev Drug Discov 2013; 12: 917-930.

[4] Wang Y, Zhang H, Chen Y, Sun Y, Yang F, Yu W, Liang J, Sun L, Yang X, Shi L, Li R, Li Y, Zhang Y, Li Q, Yi X and Shang Y. LSD1 is a subunit of the NuRD complex and targets the metastasis programs in breast cancer. Cell 2009; 138: 660-672.

[5] Lv T, Yuan D, Miao X, Lv Y, Zhan P, Shen X and Song Y. Over-expression of LSD1 promotes proliferation, migration and invasion in non-small cell lung cancer. PLoS One 2012; 7: e35065.

[6] Hayami S, Yoshimatsu M, Veerakumarasivam A, Unoki M, Iwai Y, Tsunoda T, Field HI, Kelly JD, Neal DE, Yamaue H, Ponder BA, Nakamura Y and Hamamoto R. Overexpression of the JmjC histone demethylase KDM5B in human carcinogenesis: involvement in the proliferation of cancer cells through the E2F/RB pathway. Mol Cancer 2010; 9: 59.

[7] Roesch A, Becker B, Schneider-Brachert W, Hagen I, Landthaler M and Vogt T. Re-expression of the retinoblastoma-binding protein 2-homolog 1 reveals tumor-suppressive functions in highly metastatic melanoma cells. J Invest Dermatol 2006; 126: 1850-1859.

[8] Zeng J, Ge Z, Wang L, Li Q, Wang N, Bjorkholm M, Jia J and Xu D. The histone demethylase RBP2 Is overexpressed in gastric cancer and its inhibition triggers senescence of cancer cells. Gastroenterology 2010; 138: 981-992.

[9] Liang X, Zeng J, Wang L, Shen L, Li S, Ma L, Ci X, Yu J, Jia M, Sun Y, Liu Z, Liu S, Li W, Yu H, Chen C and Jia J. Histone demethylase RBP2 induced by Helicobactor pylori CagA participates in the malignant transformation of gastric epithelial cells. Oncotarget 2014; 5: 5798-5807.

[10] Liang X, Zeng J, Wang L, Shen L, Ma X, Li S, Wu Y, Ma L, Ci X, Guo Q, Jia M, Shen H, Sun Y, Liu Z, Liu S, Li W, Yu H, Chen C and Jia J. Histone demethylase RBP2 promotes malignant progression of gastric cancer through TGF-beta1-(p-Smad3)-RBP2-E-cadherin-Smad3 feedback circuit. Oncotarget 2015; 6: 17661-17674.

[11] Li W, Zhao L, Zang W, Liu Z, Chen L, Liu T, Xu D and Jia J. Histone demethylase JMJD2B is required for tumor cell proliferation and survival and is overexpressed in gastric cancer. Biochem Biophys Res Commun 2011; 416: 372-378.

[12] Zhao L, Li W, Zang W, Liu Z, Xu X, Yu H, Yang Q and Jia J. JMJD2B promotes epithelial-mesenchymal transition by cooperating with beta-catenin and enhances gastric cancer metastasis. Clin Cancer Res 2013; 19: 6419-6429.

[13] Klose RJ, Kallin EM and Zhang Y. JmjC-domain-containing proteins and histone demethylation. Nat Rev Genet 2006; 7: 715-727.
[14] Wang Q, Ma S, Song N, Li X, Liu L, Yang S, Ding X, Shan L, Zhou X, Su D, Wang Y, Zhang Q, Liu X, Yu N, Zhang K, Shang Y, Yao Z and Shi L. Stabilization of histone demethylase PHF8 by USP7 promotes breast carcinogenesis. J Clin Invest 2016; 126: 2205-2220.
[15] Shao P, Liu Q, Maina PK, Cui J, Bair TB, Li T, Umesalma S, Zhang W and Qi HH. Histone demethylase PHF8 promotes epithelial to mesenchymal transition and breast tumorigenesis. Nucleic Acids Res 2016; [Epub ahead of print].
[16] Ma Q, Chen Z, Jia G, Lu X, Xie X and Jin W. The histone demethylase PHF8 promotes prostate cancer cell growth by activating the oncomiR miR-125b. Onco Targets Ther 2015; 8: 1979-1988.
[17] Tong D, Liu Q, Liu G, Yuan W, Wang L, Guo Y, Lan W, Zhang D, Dong S, Wang Y, Xiao H, Mu J, Mao C, Wong J and Jiang J. The HIF/PHF8/AR axis promotes prostate cancer progression. Oncogenesis 2016; 5: e283.
[18] Zhu G, Liu L, She L, Tan H, Wei M, Chen C, Su Z, Huang D, Tian Y, Qiu Y, Liu Y and Zhang X. Elevated expression of histone demethylase PHF8 associates with adverse prognosis in patients of laryngeal and hypopharyngeal squamous cell carcinoma. Epigenomics 2015; 7: 143-153.
[19] Ma L, Zeng J, Guo Q, Liang X, Shen L, Li S, Sun Y, Li W, Liu S, Yu H, Chen C and Jia J. Mutual amplification of HNF4alpha and IL-1R1 composes an inflammatory circuit in Helicobacter pylori associated gastric carcinogenesis. Oncotarget 2016; 7: 11349-11363.
[20] Szasz AM, Lanczky A, Nagy A, Forster S, Hark K, Green JE, Boussioutas A, Busuttil R, Szabo A and Gyorffy B. Cross-validation of survival associated biomarkers in gastric cancer using transcriptomic data of 1,065 patients. Oncotarget 2016; 7: 49322-49333.
[21] Xu L, Wu W, Cheng G, Qian M, Hu K, Yin G and Wang S. Enhancement of Proliferation and Invasion of gastric cancer cell by KDM5C Via Decrease in p53 expression. Technol Cancer Res Treat 2016; [Epub ahead of print].
[22] Zhu Z, Wang Y, Li X, Wang Y, Xu L, Wang X, Sun T, Dong X, Chen L, Mao H, Yu Y, Li J, Chen PA and Chen CD. PHF8 is a histone H3K9me2 demethylase regulating rRNA synthesis. Cell Res 2010; 20: 794-801.
[23] Liu Z, Li Q, Li K, Chen L, Li W, Hou M, Liu T, Yang J, Lindvall C, Bjorkholm M, Jia J and Xu D. Telomerase reverse transcriptase promotes epithelial-mesenchymal transition and stem cell-like traits in cancer cells. Oncogene 2013; 32: 4203-4213.
[24] Danesh J. Helicobacter pylori infection and gastric cancer: systematic review of the epidemiological studies. Aliment Pharmacol Ther 1999; 13: 851-856.
[25] Nam KT, Hahm KB, Oh SY, Yeo M, Han SU, Ahn B, Kim YB, Kang JS, Jang DD, Yang KH and Kim DY. The selective cyclooxygenase-2 inhibitor nimesulide prevents Helicobacter pylori-associated gastric cancer development in a mouse model. Clin Cancer Res 2004; 10: 8105-8113.
[26] Fullgrabe J, Kavanagh E and Joseph B. Histone onco-modifications. Oncogene 2011; 30: 3391-3403.
[27] Mazur PK, Reynoird N, Khatri P, Jansen PW, Wilkinson AW, Liu S, Barbash O, Van Aller GS, Huddleston M, Dhanak D, Tummino PJ, Kruger RG, Garcia BA, Butte AJ, Vermeulen M, Sage J and Gozani O. SMYD3 links lysine methylation of MAP3K2 to Ras-driven cancer. Nature 2014; 510: 283-287.
[28] Pei Y, Liu KW, Wang J, Garancher A, Tao R, Esparza LA, Maier DL, Udaka YT, Murad N, Morrissy S, Seker-Cin H, Brabetz S, Qi L, Kogiso M, Schubert S, Olson JM, Cho YJ, Li XN, Crawford JR, Levy ML, Kool M, Pfister SM, Taylor MD and Wechsler-Reya RJ. HDAC and PI3K antagonists cooperate to inhibit growth of MYC-driven medulloblastoma. Cancer Cell 2016; 29: 311-323.
[29] Xiang Y, Zhu Z, Han G, Lin H, Xu L and Chen CD. JMJD3 is a histone H3K27 demethylase. Cell Res 2007; 17: 850-857.
[30] Ntziachristos P, Tsirigos A, Welstead GG, Trimarchi T, Bakogianni S, Xu L, Loizou E, Holmfeldt L, Strikoudis A, King B, Mullenders J, Becksfort J, Nedjic J, Paietta E, Tallman MS, Rowe JM, Tonon G, Satoh T, Kruidenier L, Prinjha R, Akira S, Van Vlierberghe P, Ferrando AA, Jaenisch R, Mullighan CG and Aifantis I. Contrasting roles of histone 3 lysine 27 demethylases in acute lymphoblastic leukaemia. Nature 2014; 514: 513-517.
[31] Hanahan D and Weinberg RA. Hallmarks of cancer: the next generation. Cell 2011; 144: 646-674.
[32] Nieto MA, Huang RY, Jackson RA and Thiery JP. Emt: 2016. Cell 2016; 166: 21-45.
[33] Ryu HS, Park DJ, Kim HH, Kim WH and Lee HS. Combination of epithelial-mesenchymal transition and cancer stem cell-like phenotypes has independent prognostic value in gastric cancer. Hum Pathol 2012; 43: 520-528.
[34] Kawazu M, Saso K, Tong KI, McQuire T, Goto K, Son DO, Wakeham A, Miyagishi M, Mak TW and Okada H. Histone demethylase JMJD2B functions as a co-factor of estrogen receptor in breast cancer proliferation and mammary gland development. PLoS One 2011; 6: e17830.

[35] Yang F, Sun L, Li Q, Han X, Lei L, Zhang H and Shang Y. SET8 promotes epithelial-mesenchymal transition and confers TWIST dual transcriptional activities. EMBO J 2012; 31: 110-123.

[36] Byles V, Zhu L, Lovaas JD, Chmilewski LK, Wang J, Faller DV and Dai Y. SIRT1 induces EMT by cooperating with EMT transcription factors and enhances prostate cancer cell migration and metastasis. Oncogene 2012; 31: 4619-4629.

[37] Ghahhari NM and Babashah S. Interplay between microRNAs and WNT/beta-catenin signalling pathway regulates epithelial-mesenchymal transition in cancer. Eur J Cancer 2015; 51: 1638-1649.

[38] Sanchez-Tillo E, de Barrios O, Siles L, Cuatrecasas M, Castells A and Postigo A. beta-catenin/TCF4 complex induces the epithelial-to-mesenchymal transition (EMT)-activator ZEB1 to regulate tumor invasiveness. Proc Natl Acad Sci U S A 2011; 108: 19204-19209.

[39] Conacci-Sorrell M, Simcha I, Ben-Yedidia T, Blechman J, Savagner P and Ben-Ze'ev A. Autoregulation of E-cadherin expression by cadherin-cadherin interactions: the roles of beta-catenin signaling, slug, and MAPK. J Cell Biol 2003; 163: 847-857.

[40] Masutomi K, Yu EY, Khurts S, Ben-Porath I, Currier JL, Metz GB, Brooks MW, Kaneko S, Murakami S, DeCaprio JA, Weinberg RA, Stewart SA and Hahn WC. Telomerase maintains telomere structure in normal human cells. Cell 2003; 114: 241-253.

[41] Hartgrink HH, Jansen EP, van Grieken NC and van de Velde CJ. Gastric cancer. Lancet 2009; 374: 477-490.

[42] Han F, Ren J, Zhang J, Sun Y, Ma F, Liu Z, Yu H, Jia J and Li W. JMJD2B is required for Helicobacter pylori-induced gastric carcinogenesis via regulating COX-2 expression. Oncotarget 2016; 7: 38626-38637.